Received: 23 July 2024 | Revised: 29 October 2024 | Accepted: 31 October 2024

DOI: 10.1002/esp.6030

RESEARCH ARTICLE

ESPL WILEY

Controls on glacial kettle morphology

Jillian S. Prescott[1] | Lucas K. Zoet[1] | Dougal D. Hansen[1] | Shanti B. Penprase[2] | J. Elmo Rawling III[3]

[1]Department of Geoscience, University of Wisconsin-Madison, Madison, Wisconsin, USA

[2]Department of Earth Sciences, Dartmouth College, Hanover, New Hampshire, USA

[3]Wisconsin Geological and Natural History Survey, University of Wisconsin-Madison, Madison, Wisconsin, USA

Correspondence
Jillian S. Prescott, Department of Geoscience, University of Wisconsin-Madison, 1215 W. Dayton, Madison, WI, USA.
Email: jsprescott@wisc.edu

Funding information
We received funding from NSF grant number NSF-EAR 2218463.

Abstract

Glacial kettles are surficial depressions that form in formerly glaciated terrain when buried stagnant ice melts within pro-glacial sediments, often deposited by meltwater streams. Kettles, like other glacial landforms, provide insight into the impact of climate on landscape evolution, such as the extent and timing of glaciations. The geometry of kettle features is variable, but existing theory does not explain the range of observed morphologies. Our study aims to establish a quantitative relationship between the depth of ice burial and the resulting morphology of terrain collapse in kettle depressions. To do so, we simulated kettle formation in the laboratory by burying ice spheres of four sizes in well-sorted coarse sand at four different depths. As the spheres melt at room temperature, a glacial kettle analog forms at the surface. We scanned the resulting kettle topography with a portable LiDAR scanner to produce 3D digital elevation models of each depression, from which we measured each depression's depth and width and, in one instance, the time series of kettle formation. Using this data, we quantified the relationship between the sphere diameter, burial depth and resulting dimensions of the kettle by developing a set of equations, which we then applied to full-scale features. Our results indicate that ice burial deeper than one sphere diameter corresponds to a decrease in depression depth and an increase in depression width. This application offers insight into the interdependence of ice burial depth and kettle geometry.

KEYWORDS
burial depth, kettle formation, kettle morphology, landscape evolution, melt out

1 | INTRODUCTION

As glacial margins retreat, ice frequently breaks off from the terminus of the glacier, often due to a combination of decreasing ice thickness, meltwater interaction and basal friction (Hooke, 2019). The margin properties—such as steepness, advancing versus retreating status and internal temperature structure—will all affect the size and distribution of ice blocks that shed off the front of glaciers. When ice blocks separate from a land-terminating glacier, they are often buried by glacial deposits like glaciofluvial sediments (Benn & Evans, 2014). Icebergs may also be transported onto glaciofluvial outwash plains by floodwaters, particularly during Jökulhlaups (Burke et al., 2010) where they are subsequently buried by outwash sediments. While the ice blocks are whole, these sediments create a continuous, nearly flat surface. Over time, however, the buried ice blocks melt, forming voids at depth and disrupting the continuous surface. Eventually, these growing voids at depth cause the sediment surfaces to collapse. These collapses create depressions on the landscape, called kettles, which reflect the burial and melt-out processes that occurred. Kettles exhibit a diverse range of shapes but are generally circular, and they frequently populate pro-glacial outwash plains (Figure 1). Kettles in formerly glaciated landscapes vary widely in width and depth, ranging from 5 to 13 km in diameter and achieving depths of up to 45 m (Flint, 1971).

Once a depression has formed, it can fill with water. This often occurs when the base of the kettle lake intersects with the water table, allowing groundwater to fill the depression, but it may also fill from accumulating surface water (Kentula, 1989). In either case, a

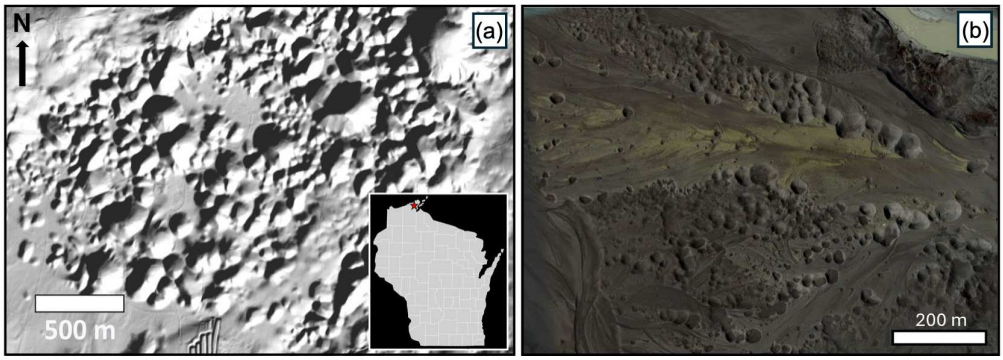

FIGURE 1 Naturally occurring kettles. (a) Terrain shaded relief map generated from a digital elevation model (DEM) derived from light detection and ranging (LiDAR) data of dry kettles in Bayfield County, WI. (b) Aerial photo of a range of kettles near Skeiðarárjökull glacier in Iceland, captured via Google Earth satellite. [Color figure can be viewed at wileyonlinelibrary.com]

kettle filled with water is called a kettle lake. The paleoclimatic record can be explored by analyzing the organic material collected from kettle lake cores (Yansa et al., 2020). However, organic material does not provide information about the initial formation of the kettle, such as the factors that defined its depth and width—a key aspect of kettle lakes that remains poorly understood.

Kettles not only provide insights into the past but they also hold modern significance. Environmentally, kettle lakes represent one of the largest and most hydrologically diverse groups of inland wetlands (Gleason et al., 2011). The isolation of these kettle wetlands creates a microclimate that serves as a refuge for vulnerable species (Gerke et al., 2010) and fosters unique ecosystems. These ecosystems, in turn, influence local flora and fauna, thereby promoting biodiversity. Societally, kettle lakes are also important. Communities that live in deglaciated areas are often dependent on kettle lakes because they provide resources like a water supply for agriculture (Vasić et al., 2020).

Previous research has established the basic mechanisms behind kettle formation and explored the factors contributing to kettle geometry. Maizels (1977) confirmed the assumption that kettles form from the melting of buried ice through laboratory experiments. These experiments tested multiple theories of kettle formation and found that the depressions made by melting buried ice most closely resembled the physical characteristics of natural kettles. In addition, Maizels (1977) demonstrated that the size of a kettle is dependent on the depth at which the ice is buried; however, Maizels (1977) focused on a qualitative description of this concept without establishing a quantitative relationship. Maizels ([1977]) showed that kettle structure is also dependent on the volume of sediment contained within the melting ice block. Ice blocks that contain more sediment produce kettles with boulder-rich, ringlike ridges on the edges of the depression (Maizels, 1997). Lolos (2013) also explored the relationship between ice blocks and the resulting depression using physical experiments and digital models. This study quantified the volume of material transferred into the void formed through the melting ice block and documented the alterations to the surrounding sediment. Overall, studies have qualitatively linked kettle morphology to the dimensions of ice and the depth of burial, but more research is needed to understand and quantitatively define how formation conditions dictate kettle morphology.

The role of kettles as part of the regional ground and surface water hydrology has spurred investigations into kettle lakes, including the factors that lead a kettle to develop into a wetland environment (Götz et al., 2018) and their modern environmental significance (Gerke et al., 2010; Gleason et al., 2011). Götz et al. (2018) used a variety of electrical geophysical methods to probe the base and regions surrounding kettle lakes, observing both the organic material accumulating at the base of the lake and the till or outwash that lay beneath the lakebed. In several instances, they found a zone of high electrical resistivity atop a zone of low electrical resistivity within the outwash sediments beneath the lake base. As electrical resistivity is often inversely related to sediment porosity, their findings indicate that some kettle lakes have a zone of low porosity situated atop a zone of high porosity within the sediments. The porosity of the sediments surrounding the lake, along with the overall shape of the lake, will directly affect the ability for groundwater to flow into and out of the lake, thus altering the limnology. Given our current understanding of kettle depression formation, it is unclear what effects the melt-out process may have on the overall shape of the kettle and the hydrological properties of the surrounding sediments.

Despite the prevalence of kettles on the glacial landscape, the specific formation conditions that dictate their morphology are not fully understood. To better understand kettle formation and the factors contributing to variations in kettle geometry, we ran a series of laboratory-based experiments. Using ice spheres of four different volumes and a sandbox apparatus, we simulated kettle formation under four different burial depths. Analyzing how the depth and width of the depressions changed with increasing burial depth for four different sphere volumes revealed relationships between kettle geometry and ice sphere volume and burial depth, respectively. We then compared these results to kettle depressions on a postglacial landscape in Wisconsin to assess the validity of the equations we developed from our experiments. Our study establishes the first quantitative relationship between the ice burial depth, the ice block size and the resulting depression's depth and width.

2 | METHODS

2.1 | Lab experiments

To simulate kettle formation in the lab, we first froze water in a spherical silicon mold, using four different silicon molds that generated ice

spheres with four different diameters (4, 6, 7 and 10 cm). The resulting ice sphere was then buried in a container (72.4 × 49.8 × 38.6 cm) of well-sorted dry coarse sand (modal grain diameter of 0.778 mm). Each size of sphere was buried at four different depths, *Z*, to examine the effect of burial depth on depression morphology, for a total of 16 different experiments. The four burial depths were standardized based on the radius of the spheres, denoted herein as 'half-', 'full-', 'double-' and 'triple-buried' (Figure 3a). Half-buried refers to experiments in which the bottom of the ice sphere reached one radius distance below the sand's upper surface so that half of the ice sphere was protruding above the sand surface (Figure 2). For full-buried depth, the bottom of the sphere reached one diameter's distance below the surface so that none of the ice could be seen above the surface. Double- and triple-buried meant that the bottom of the sphere was two and three diameters below the sand surface, respectively. We chose sand specifically as the burial medium for two reasons: (1) many kettles are found in outwash comprised of sand-sized particles, and (2) sand generally lacks cohesion as a factor in its shear strength. This allowed the experiments to be more generalizable to larger scale field observations where the effects of cohesion on morphology development would be minimized relative to the lab scale. We also note that the sand used for these experiments was collected from our field area in Bayfield County, Wisconsin, where numerous kettles are located, making it a realistic sediment in which kettles form. The sand's upper surface was leveled by hand using a flat object after each sphere was buried. The sand was intentionally not packed or compressed during the burial or leveling process. The ice was then left to fully melt at room temperature without disruption. To ensure that the depression reflected ice that had entirely melted, the experiment was left for at least 8 h. As the ice sphere melts, the highly permeable sand allows the meltwater to flow down the steepest hydropotential gradient, which is vertical in our experiments due to the absence of a water table or surface slope. It takes in excess of 6 h for the ice block to melt. Given the high permeability and the relatively slow rate of melt, the transmissivity of the sediment was sufficient to ensure all melt water flowed effectively vertically toward the base of the container without ponding around the melting sphere. Between each ice sphere burial, the sand was allowed to dry completely to prevent any moisture from affecting the sediment's cohesion and, consequently, the shape of the depression. In one additional experiment, a 10-cm sphere was full-buried, and the resultant depression morphology was measured every 30 min for a total duration of 6.5 h. This experiment provided insights into the time-dependent evolution of depression morphology during the melt-out process.

FIGURE 2 Profile image of a 10-cm ice sphere half-buried within a container of well-sorted, coarse sand. The bottom of the ice sphere is positioned at a depth equal to one radius (5 cm) below the sand surface, with approximately half the sphere protruding above the sand surface. [Color figure can be viewed at wileyonlinelibrary.com]

For each melted ice sphere, a three-dimensional scan of the sand's depressed surface was collected using a NextEngine Ultra HD 3D scanner and ScanStudio software (Figure 3b). To capture the entire kettle depression, the scanner was set to 'wide lens' mode and oriented normal to the surface at ~70 cm. These settings resulted in an accuracy of 0.0149 mm, estimated by measuring the deviation of a scan taken of a precisely flat manufactured rock slab from a perfectly flat plane. Due to the darker tone of the sand, the 'dark subject' setting was utilized. The scans were converted to XYZ files, from which a

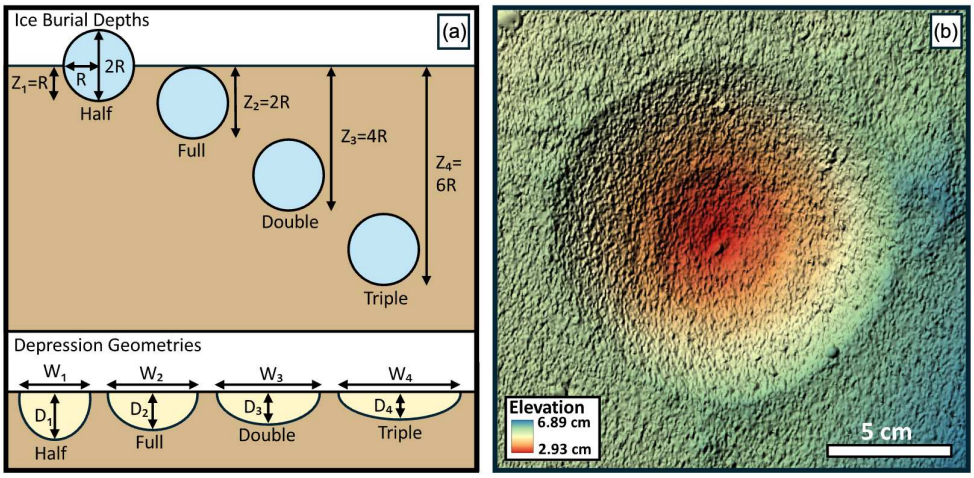

FIGURE 3 (a) Conceptual diagram of the four burial depths (half, full, double and triple) used in the experiments. The diagram shows that with progressively deeper burial, the resulting kettle's depth decreased, while the width increased. (b) DEM of a full-buried 10 cm ice sphere. For each experiment that was done a DEM was created from the 3D scan of the sand's surface. [Color figure can be viewed at wileyonlinelibrary.com]

Digital Elevation Model (DEM) was created in QGIS to constrain the depression morphology (Figure 3b). On each DEM, four elevation profiles were made along four different transects that were taken at even intervals around the circular depression, and the same four positions were used for all depressions. Using these elevation profiles, we measured the depth and width of the depressions. Depth, *D*, was defined as the distance from the lowest point on the profile to the mean elevation of the horizontal sand surface, while width, *W*, was measured across the depression from one break in the slope to the opposite break (Figure 4a). The average depth and width were calculated from the four profiles collected from each DEM. From these averages, we estimated a proxy for 2D volume (*D*·*W*) and the aspect ratio (*D*/*W*). We chose these shape metrics because they are relatively easy to obtain when measuring natural field depressions.

2.2 | Field observations

For our field data analysis, we focused on a region on the Bayfield Peninsula in Wisconsin (Figure 1a), where numerous kettles formed as the Lake Superior Lobe of the Laurentide Ice Sheet retreated from the Bayfield Highlands. Their formation coincided with the final phase of

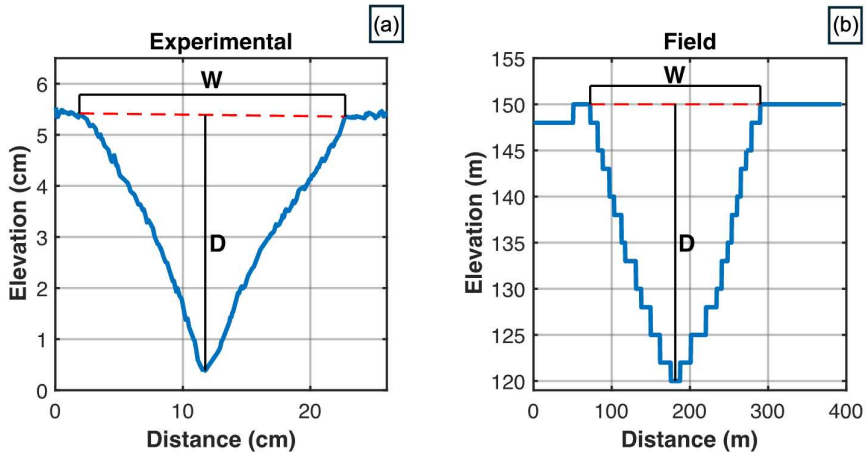

FIGURE 4 Conceptual diagram of elevation profiles used to determine depression dimensions. (a) Experimental kettle: Depth is measured from the lowest point to the mean elevation of the surrounding semi-flat sand surface. Width is measured between opposite breaks in slope. (b) Natural kettle in Bayfield County, WI: Depth is measured from the lowest point to the mean elevation between two opposite breaks in slope when kettles are overlapping and a flat surface is unclear, and width is measured using the same procedure as experimental kettles. The y-axis in this figure is vertically exaggerated, making the kettle appear very deep and narrow, but without exaggeration the kettle is relatively wide and shallow. [Color figure can be viewed at wileyonlinelibrary.com]

TABLE 1 Summary of sphere radius, burial depth, depression dimensions, aspect ratios and 2D volume for the 16 experiments conducted.

Ice SphereRadius (cm)	Ice sphere burial depth (cm)	Resulting depression depth (cm)	Resulting depression width (cm)	Resulting aspect ratio (D/W) (--)	Resulting 2D volume (D × W) (cm^2)
2	2	1.34	6.42	0.21	8.60
2	4	1.61	8.53	0.18	13.74
2	8	1.58	10.09	0.16	15.98
2	12	0.81	17.86	0.05	14.55
3	3	2.48	10.03	0.25	24.90
3	6	2.62	12.56	0.21	32.94
3	12	1.68	12.61	0.13	21.25
3	18	1.08	17.61	0.06	19.07
3.5	3.5	2.84	11.28	0.25	32.12
3.5	7	3.37	14.79	0.23	49.88
3.5	14	1.68	14.10	0.12	23.65
3.5	21	1.29	18.27	0.07	23.62
5	5	2.74	14.17	0.19	38.83
5	10	5.00	0.24	0.24	103.53
5	20	2.62	14.64	0.18	38.36
5	30	2.06	17.16	0.12	35.43

retreat during the Wisconsin Glaciation, when the Lake Superior Lobe advanced and retreated in Wisconsin multiple times between approximately 31.5 and 11 ka before present (Mickelson & Attig, 2017). Due to the Bayfield Peninsula's relatively high elevation compared to the adjacent landscape and the sandy outwash in which the kettles formed, the local water table lies hundreds of meters below the base of the kettles, rendering them devoid of water or 'dry' (Fehling et al., 2022). While less common, dry kettles are ideal for our purposes as they allow us to easily estimate depth (*D*) from LiDAR data, which cannot penetrate water in kettle lakes. These kettles have likely experienced some changes from hillslope processes after their formation. However, because the slopes are relatively shallow and they are not filled with water, their alterations are minimal compared to other kettles. The LiDAR data from this region has a roughly 1.5-m horizontal resolution and is publicly available (Wisconsin State Cartographer's Office, 2023).

In this region, we identified 88 distinct kettles. Each kettle was measured with four elevation profiles, using the same method as the experimental data, to estimate their average depth and width. Calculating an average was particularly important for the field data due to the nonuniform shape of the kettles, caused by their overlap with one another. Following a similar process as the experimental data, width was measured across the depression from one break in slope to the diametrically opposed break in the slope (Figure 4b). However, due to the overlapping of kettles in some situations, there was not an extended flat surface surrounding the kettle that could be used as a border for the top of the depression. In those instances, the depth was measured from the lowest point on the elevation profile to the mean elevation between the two opposite breaks in slope. The shapes of the kettles were also graded based on the level of interference with nearby kettles (Figure S3). A kettle with a ranking of 5 indicates that no other kettles overlap it, while a kettle with a ranking of 1 indicates that at least 4 kettles overlap its perimeter.

3 | RESULTS

3.1 | Experimental results

Table 1 gives the dimensions of each experimental kettle, and Figure 5 shows the relationships between the aspect ratio and 2D volume with nondimensionalized burial depth (*Z*), respectively. We normalized *Z* by sphere diameter (2*R*, where *R* is radius) to scale the results and enable comparison between the different sphere sizes. We find that as the depth of burial increased, the resulting depression generally decreased in *D* and increased in *W*. For all four diameter sizes, the depth of the depression of the double-buried sphere ($Z/2R = 2$) was less than that of the full-buried ice sphere ($Z/2R = 1$). Interestingly, the peak 2D volume ($D{\cdot}W$) was observed in all cases when the sphere was full-buried (Figure 5b), exhibiting a non-monotonic response in which volume decreased with both shallower and deeper burial than full-burial. The aspect ratio (D/W) continually decreased with increasing burial depth ($Z/2R$) (Figure 5a). In summary, when the ice was buried deeper, the ratio of depth to width of the depression decreased. For three out of the four ice sphere sizes,

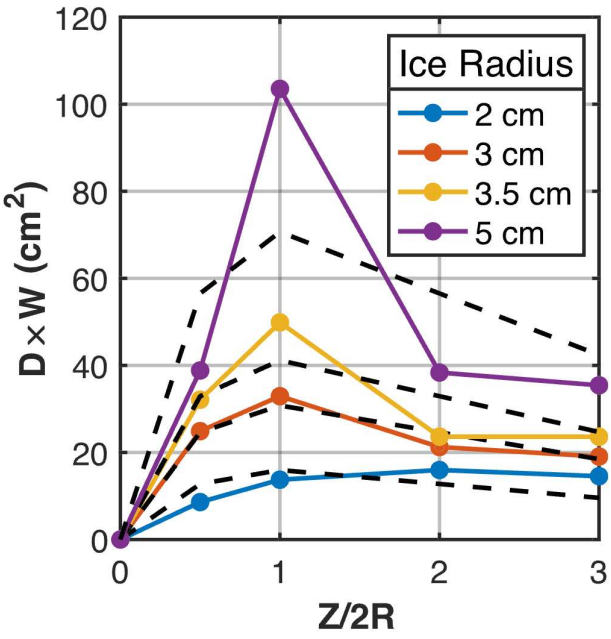

FIGURE 6 Non-monotonic model best fit to the relationship between 2D volume and normalized burial depth. The function fit to this data is $b \cdot \left(\frac{x}{x^2+1}\right)$, where *x* represents the normalized burial depth and *b* is the appropriate coefficient for the fit. [Color figure can be viewed at wileyonlinelibrary.com]

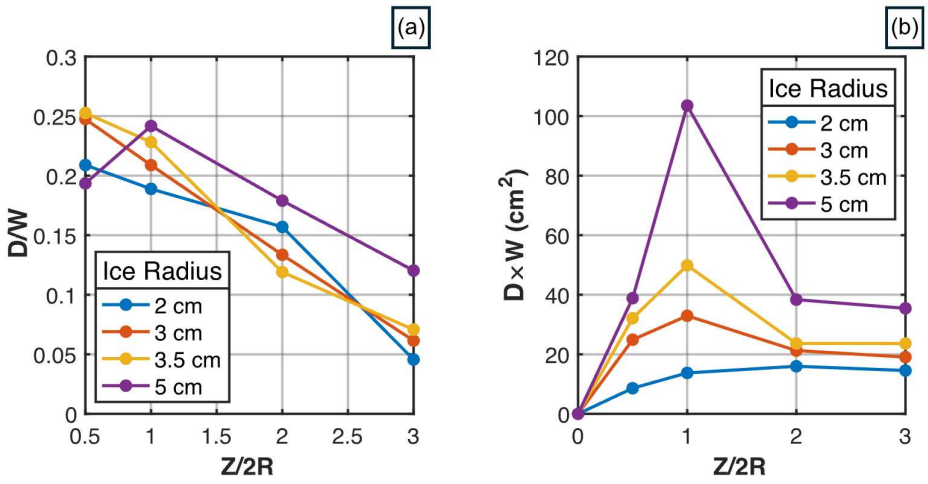

FIGURE 5 Relationships between aspect ratio and 2D volume with nondimensionalized burial depth. (a) Aspect ratio as a function of nondimensionalized burial depth. This diagram shows that the aspect ratio decreases continuously with increasing burial depth. (b) 2D volume as a function of nondimensionalized burial depth, demonstrates a non-monotonic relationship, with full burial showing the largest 2D volume. [Color figure can be viewed at wileyonlinelibrary.com]

the aspect ratio was largest when the ice was half-buried ($Z/2R = 0.5$) (Figure 5).

From these observations, we generated functions that estimate the 2D volume and aspect ratio of a depression from the radius and burial depth of the sphere (Equations 1 and 2, respectively; Figure 6). For the 2D volume, the non-monotonic equation includes a single fitting parameter, m, that scales the amplitude of the function, which we found to be consistent between all sphere sizes ($m \sim 5$) (Figure S1). The aspect ratio was well-described by a function dependent on the nondimensionalized burial depth, exhibiting a linear decrease with a

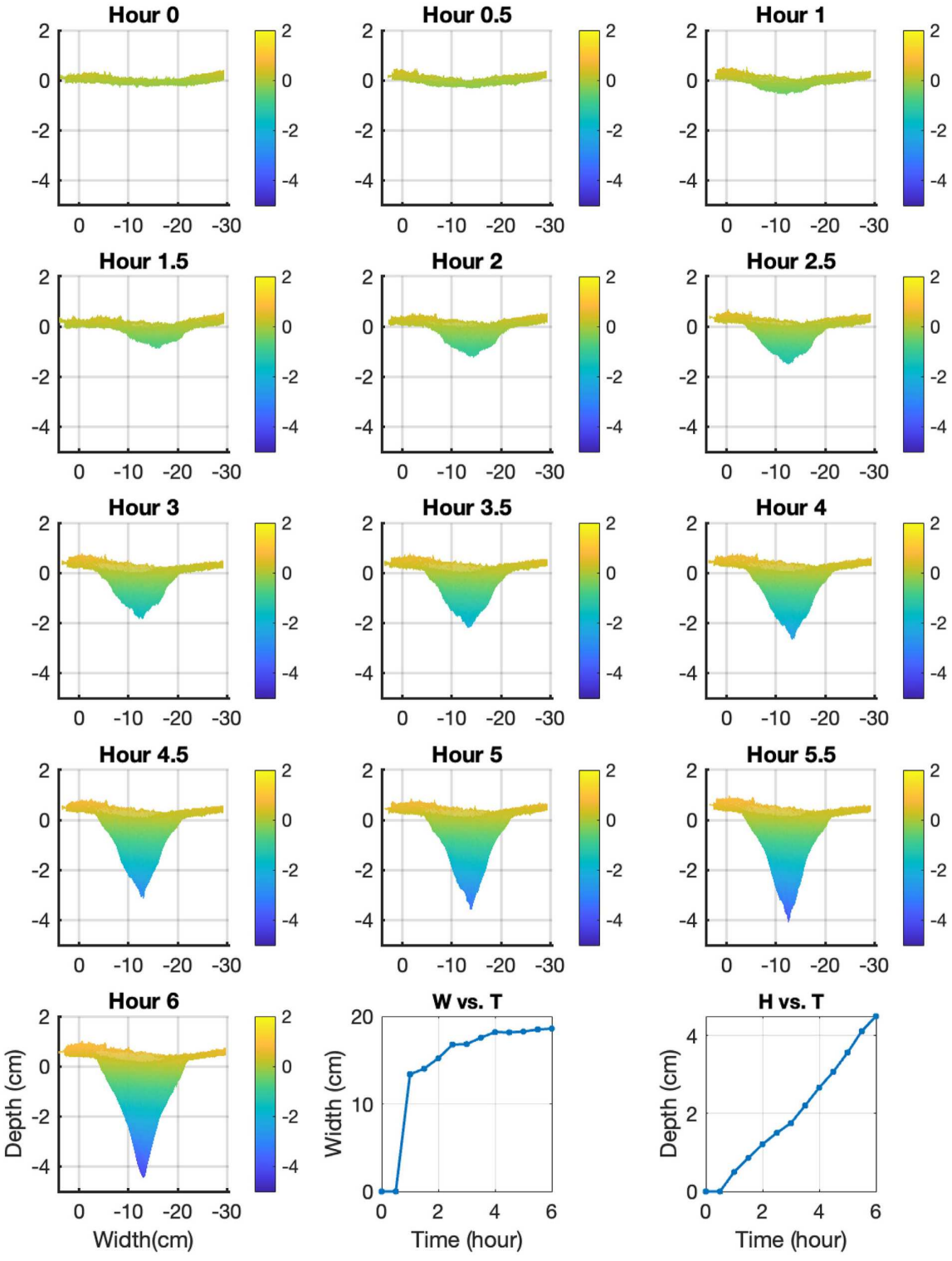

FIGURE 7 Time-lapse sequence showing the formation of a kettle from a full-buried 10 cm ice sphere over a 6.5-h period. The absolute dimensions evolve over time, which supports lateral sediment transfer during melt out. The color bar is elevation relative to the average original surface height in cm. [Color figure can be viewed at wileyonlinelibrary.com]

slope $l = -0.65$ from a vertical offset $c = 0.27$ (Figure S2). The values of l and c were again consistent between all sphere sizes, bolstering confidence in their scalability. Importantly, these two relationships can be solved together numerically, assuming a spherical ice block, to estimate Z and R from depressions on the landscape. Note that a simple analytical solution was not found, so the solution required a numerical solution.

$$D \cdot W = mR^2 \left(\frac{Z/2R}{1+(Z/2R)^2} \right), \quad (1)$$

$$\frac{D}{W} = \left(\frac{Z}{2R} \right) l + c, \quad (2)$$

The time-dependent response of the system shows that the depression steadily grew with time (Figure 7). The width of the depression grew linearly for the first 2 h and then eventually approached a consistent width for the remainder of the melting time. The depth of the depression also grew linearly until it reached its final depth after ~6.5 h.

3.2 | Field results

Of the 88 kettle depressions identified in the Bayfield Lidar data, kettle widths ranged from 26 to 347 m (average width, $W_{avg} = 114$ m), and depths ranged from 3 to 38 m (average depth, $D_{avg} = 13$ m). This variation resulted in a wide range of aspect ratios. To ensure that our experimental results could be scaled up to the size of naturally occurring kettles, we compared the aspect ratios between the experiments and the field data. We found that our field and experimental aspect ratios overlap, providing more confidence in the scalability of these results (Figure 8); 100% of the Bayfield kettles' aspect ratios fall within the experimental aspect ratios and the interquartile ranges have 61% overlap. Specifically, the middle 50% of the Bayfield kettles' aspect ratios were between the values of 0.1 and 0.15, while the middle 50% of the experimental aspect ratios ranged from 0.12 to 0.22. We found that for the grade 5 kettles ($n = 11$), $W_{avg} = 76$ m and $D_{avg} = 8.5$ m, and for the combined grade 4 and 5 kettles ($n = 47$), $W_{avg} = 109$ m and $D_{avg} = 12.4$ m (Figure 9a). Using Equations 1 and 2, we can estimate the Z and R needed to produce kettles with these dimensions (Figure 10). For the grade 5 kettles, the ice sphere would have had a radius of ~35 m and had its base buried to a depth of 85 m (so roughly 50 m of sediment atop the ice sphere). In this location, the depth of the outwash is ~120 m (Fehling et al., 2022). Estimates of Z and R from the solutions of Equations 1 and 2 for all five grades are plotted in Figure 9b.

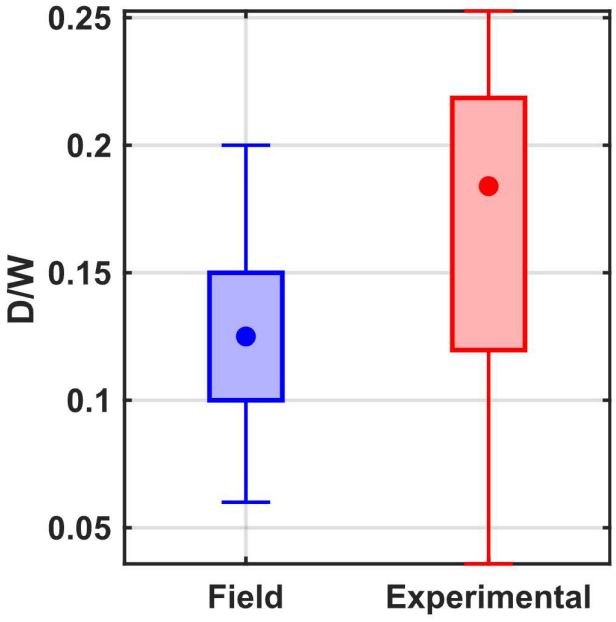

FIGURE 8 Box and whisker plot comparing the distribution aspect ratios for field and experimental kettles. The box indicates the interquartile range, where 50% of the data is found, and the whiskers extend from the minimum to maximum aspect ratio values for each data set. [Color figure can be viewed at wileyonlinelibrary.com]

4 | DISCUSSION

These laboratory results provide the first quantitative relationship of kettle depression geometry resulting from variation in burial depth and ice sphere size. The nondimensionalized experimental aspect ratios overlap with the aspect ratios of the natural kettle depressions. This indicates the range of parameters we have explored in the lab are possible in nature and provides confidence in the scaling of the lab results to the field scale as a first-order approximation. It was expected that the volume of the kettle depression would increase as the burial depth approached full burial, simply because the ice sphere occupies more space underneath the surface as it approaches full buried. However, interestingly, at burial depths greater than full buried, the volume of the depression decreased with increased burial depth. A potential explanation for this phenomenon is that the sediment initially situated atop and adjacent to the buried ice must undergo wide scale reorganization and deformation as it moves into the void space created by the melting ice block. This act of sediment reorganization causes the mobilized sediment to undergo repacking (e.g., grain rearrangement) as it moves into the void. As the sediment moves into the newly forming void from the region surrounding the ice block, its overburden stress (stress from the overlying sediment) is reduced from its initial condition when adjacent to the ice block. In response, the mobilized sediment attains a higher porosity after repacking because of the reduced overburden stress, following standard consolidation theory (Lambe & Whitman, 1991). This proposed increase in porosity in the zone surrounding the kettle agrees with the geophysical observation of Götz et al. (2018), who imaged a potentially low porosity zone immediately below the depression of a kettle lake. The sediment surrounding the lake, which has higher porosity, would facilitate greater permeability and groundwater flow into and out of the lake. Conversely, those ice blocks that were buried 'full' or shallower should exhibit much less or possibly no change in the porosity in the surrounding sediment as the ice block melts because little to no sediment is positioned atop the melting ice block; thus, less reorganization of sediment takes place. This leads to less hydrologic permeability and a decrease in the potential for groundwater flow into and out of lakes. In this manner, the formation mechanisms of the kettle as they relate

to a specific burial depth would directly impact the limnology of lakes that may develop within the kettles.

Solving Equations 1 and 2 together provides a means to estimate an ice block's burial depth and radius from the field data. This is possible because the burial depth and size affect the depression shape in two distinct ways. The volume of the depression scales in one manner following Equation 1 with sphere size and burial depth. By using Equation 1 in combination with a volume estimate of a depression, we can estimate a nondimensionalized burial depth, though a unique solution of R and Z does not exist from Equation 1 alone. However, by combining Equations 1 and 2 to assess D and W, we can identify a unique combination of R and Z if the buried object resembles a sphere or is roughly equant in shape (we will detail additional limitations below). Figure 10 shows the range of solutions for aspect ratio and volume. There are only a limited number of R and Z combinations that can satisfy both Equations 1 and 2 for measured D and W observations. As a sphere of a given size becomes buried deeper, the volume of the depression first increases and then decreases past the threshold of full burial. At the same time, the volume of a depression is directly proportional to the volume of the sphere for a given depth (e.g., a larger block of ice will produce a larger depression than a smaller block of ice buried at the same relative depth). However, as a sphere of a given radius is buried deeper, its aspect ratio linearly decreases, leaving a depression that becomes shallower and wider. We hypothesize that is because there is a 'cone' of effective sediment that is positioned upwards, so that the widest part of the cone is nearest to the surface, from the buried ice block at an angle related to the sediment's friction angle (Figure 11, Figure S4). Our experiments suggest a sphere buried in sediment that has a friction angle, ϕ, will affect a region at the surface, W that follows (Figure S5):

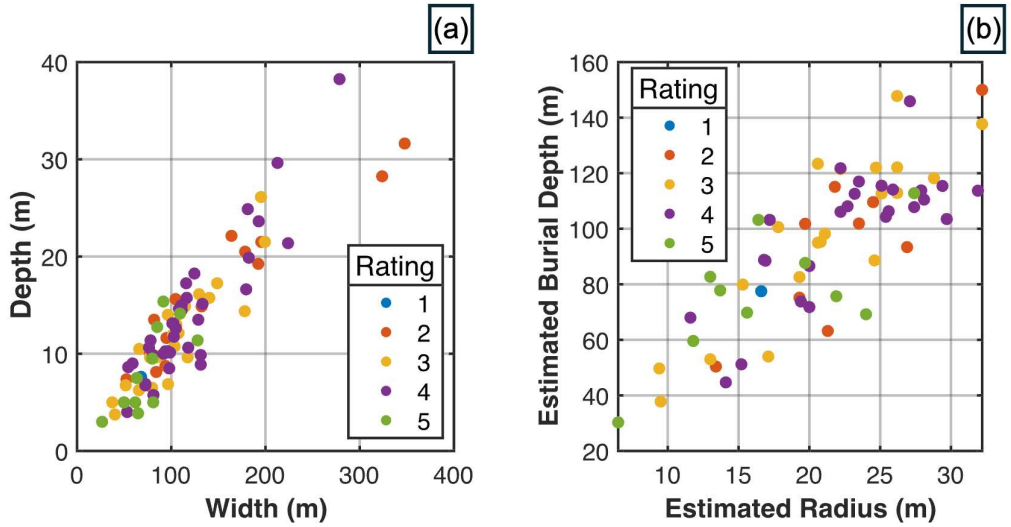

FIGURE 9 (a) Scatter plot of measured depth and width values of 88 naturally occurring kettles from Bayfield, WI, and ranked from least disrupted (5) to most disrupted (1). (b) Scatter plot of estimated ice burial depth and estimated radius calculated using Equation 1 and Equation 2. [Color figure can be viewed at wileyonlinelibrary.com]

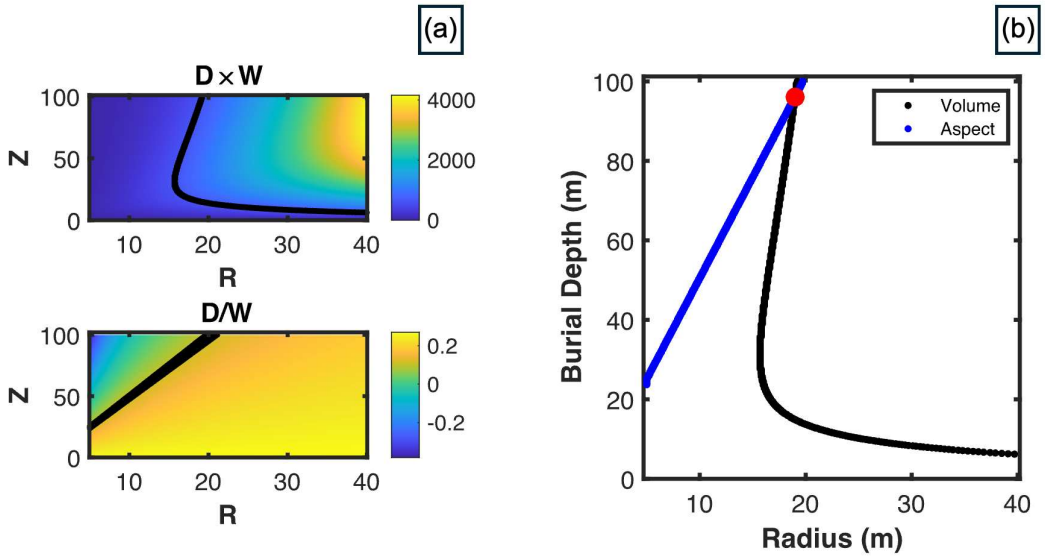

FIGURE 10 Diagrams demonstrating the numerical solution. (a) The black lines represent potential values of ice burial depth (Z) and ice radius (R) that match a kettle's calculated 2D volume and aspect ratio. (b) The intersection of the blue and black lines indicates where the potential depth and width satisfy both Equation 1 and Equation 2. [Color figure can be viewed at wileyonlinelibrary.com]

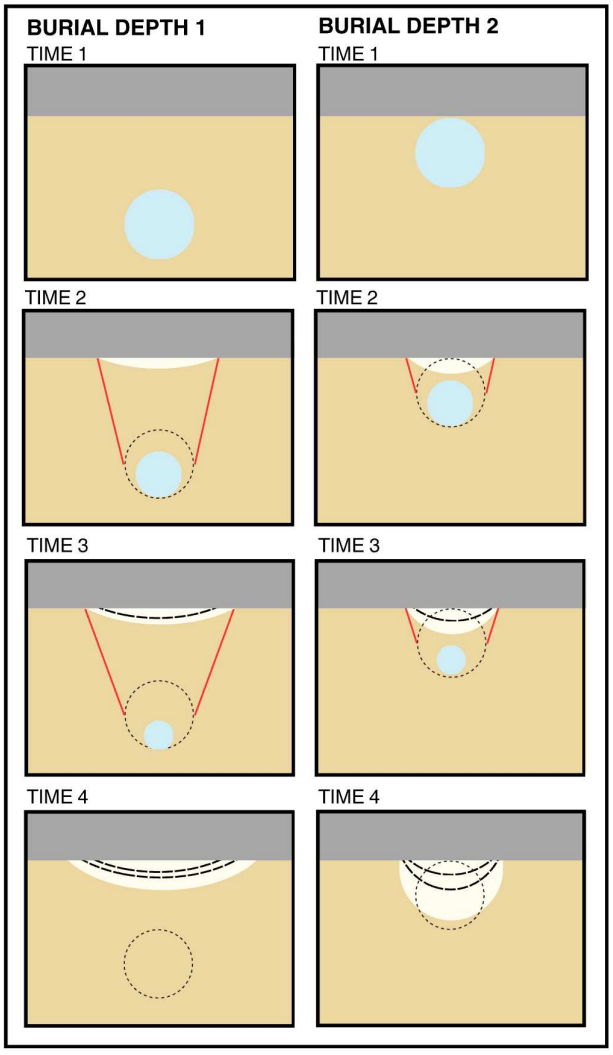

FIGURE 11 Conceptual diagram depicting the melting of ice spheres buried at two different depths and their impact on the growth and shape of the resulting depression. [Color figure can be viewed at wileyonlinelibrary.com]

$$W = \frac{2Z}{\tan(90-\phi)}. \quad (3)$$

For a sphere buried 10 m with $\phi = 30°$, this would equate to $W = 11.5$ m, whereas a sphere buried 5 m will affect a zone that is 6 m in width. At the same time, the sediment from the affected cone region must fill in the void created by the melting ice block. Therefore, the same size sphere will necessitate a greater depression, D, when buried 5 m than 10 m since the area of sediment within the affected cone is smaller for the shallower burial, and hence necessitating the resulting D value will be larger for the 5 m burial than 10 m (since sediment is being drawn in from a smaller region). An exact solution for D with Z and R is speculative due to the changing sediment porosity associated with the melt out, which does not allow volume to be conserved but should scale like the following:

$$H = \frac{\pi R^2 \tan(90-\phi)}{\alpha Z} \quad (4)$$

where α is a fitting parameter that accounts for the change in porosity associated with the sediment rearrangement. The details for deriving Equations 3 and 4 are shown in the supplemental material. We note that the expressions for D and W in Equations 3 and 4 are only applicable for ice blocks that are full-buried or deeper. The time-dependent evolution of the depression largely showed a linear change in D and W as the morphology approached the final depression geometry.

The thermodynamics of the melting sphere in the lab are likely different than those in the field. However, the time-dependent melt-out progression (Figure 7) indicates that the depression grows in a manner that is not self-similar. This means that the kettle morphology at an intermediate melt-out stage is different from the final shape of the kettle. While the $D{\cdot}W$ continues to grow with time as expected (Figure 7), interestingly, the D/W also continues to grow with time (Figure 7). This means that the final aspect ratio is not achieved until the melt out is completed. At an intermediate stage of melt-out, the aspect ratio is smaller than at the final melt out, meaning the depressions are relatively shallower and wider compared to the final aspect ratio. This suggests that kettles initially grow faster in width than they do in depth, indicating the need for sediment to be transferred laterally as melt-out occurs, which supports the general model proposed above.

These experiments are highly idealized but appear to capture important aspects of kettle formation despite their limitations. A primary concern is how well the experimental observations scale to field conditions; for example, sediment composition in the field would likely include additional grain sizes beyond sand-sized particles. Those mixtures of grain sizes would give rise to more complex interactions as the ice block melted. If there were a large component of fine-grained particles, electrostatic interactions could give rise to an appreciable cohesion component that would ultimately affect the transport of the particles during deflation. However, many kettles form in outwash deposits where much of the fine-grained particles have been removed and the composition is largely sand-sized particles (Hagg, 2022). The mechanisms by which sand-sized grains (or larger) move should not be appreciably different in the field than in our experiments. Thus, we feel the use of sand in our experiments represents a valid first approximation. In addition, the ice spheres in our experiments are orders of magnitude smaller than in a natural setting. We have attempted to limit the scale-dependent aspects via the use of sand particles (thereby reducing the importance of cohesion) and limiting the minimum size spheres we use to >10x the maximum grain size in accordance with standard soil mechanics procedures (Head, 1989). By limiting the low end of our sphere size, we have reduced some of the complexities that would arise from force chain formation and deformation mechanics as the sediment was mobilized (Hansen & Zoet, 2022). An additional limitation of our experimentation is the simplified geometry we have chosen for our ice blocks, in that they are limited to only a sphere shape. We chose a sphere as a simplified starting point, but by no means are all ice blocks spherical in shape. Our experimental results are likely reasonable for equant-shaped ice blocks (even if not spherical) but could deviate significantly if the ice blocks have one axis that is much longer than the others. This likely holds for equant shapes as any protuberances atop a sphere will have a greater surface area to volume ratio and thus melt faster than the other regions, pushing the block towards a spherical shape where this analysis is more appropriate. Further experimentation is needed to examine the complexity that non-equant shapes would impose upon the relationships we have found. Additionally, Ice blocks

that are stranded atop outwash plains (e.g., Burke et al., 2010) will require some time to be partially or fully buried and would experience syn-depositional melting. This would change the shape and size of the ice block during burial, introducing yet another complexity that warrants further investigation. Acknowledging these limitations, we believe these findings are a useful first-order approximation for how the morphology of kettle depressions relates to the ice that formed them.

5 | CONCLUSIONS

This study provides the first empirical evidence quantitatively linking the size and depth of an ice block to the morphological depression it leaves on the landscape. In our experiments, we found that the size of the ice block and the burial depth affect the aspect ratio and the volume of the depression. Specifically, the aspect ratio linearly decreases with increasing burial depth, and the volume follows a non-monotonic pattern: It increases with burial depth until the ice block is completely buried beneath the sediment surface, after which the volume decreases with increasing burial depth. The range of results found in the experiments overlaps with the range observed in nature. In addition, there is a zone of sediment that is affected by the melt out, in which sediment is mobilized and the porosity is altered, in agreement with field geophysical observations. Time-dependent melt-out measurements showed that the width of the depression initially grew faster than the depth during melt out, resulting in a depression morphology that changed significantly over time before reaching its final shape. Overall, the relationships found in this study allow us to use the dimensions of a kettle to estimate the size of the ice block and the depth at which it was buried.

ACKNOWLEDGEMENTS

The authors would like to thank Dave Lovelace for allowing us to use his NextEngine Ultra HD 3D scanner and for teaching us how to properly use it. We would also like to thank Savannah Lipinski and Jack Zoet for helping us with the experiments for this project.

CONFLICT OF INTEREST STATEMENT

None of the material has been published or is under consideration elsewhere, and there are no conflicts of interest.

DATA AVAILABILITY STATEMENT

This work was supported by NSF EAR award number 2218463 to LKZ. All data generated from this work is available at https://minds.wisconsin.edu/handle/1793/89618 and the remote sensing data can be obtained from https://www.sco.wisc.ed/data/elevationlidar/.

ORCID

Jillian S. Prescott https://orcid.org/0009-0000-0697-2458
Lucas K. Zoet https://orcid.org/0000-0002-9635-4051

REFERENCES

Benn, D. & Evans, D.J. (2014) *Glaciers and glaciation*. London: Routledge.

Burke, M.J., Woodward, J. & Russell, A.J. (2010) Sedimentary architecture of large-scale, jökulhlaup-generated, ice-block obstacle marks: examples from Skeiðarársandur, SE Iceland. *Sedimentary Geology*, 227(1–4), 1–10. Available from: https://doi.org/10.1016/j.sedgeo.2010.03.001

Fehling, A., Rawling, J., Graham, G., Chase, P., & Swanson, S. (2022) *Hydrogeology of the sandy uplands of the Bayfield Peninsula, Wisconsin*. In Open-file Report—Wisconsin Geological and Natural History Survey. Madison, WI: Wisconsin Geological and Natural History Survey. https://doi.org/10.54915/znsx3519

Flint, R.F. (1971) *Glacial and quaternary geology*. New York: John Wiley and Sons.

Gerke, H.H., Koszinski, S., Kalettka, T. & Sommer, M. (2010) Structures and hydrologic function of soil landscapes with kettle holes using an integrated hydropedological approach. *Journal of Hydrology*, 393(1–2), 123–132. Available from: https://doi.org/10.1016/j.jhydrol.2009.12.047

Gleason, R.A., Euliss, N.H., Jr., Tangen, B.A., Laubhan, M.K. & Browne, B.A. (2011) USDA conservation program and practice effects on wetland ecosystem services in the prairie pothole region. *Ecological Applications*, 21(sp1), S65–S81. Available from: https://doi.org/10.1890/09-0216.1

Götz, J., Salcher, B., Starnberger, R. & Krisai, R. (2018) Geophysical, topographic and stratigraphic analyses of perialpine kettles and implications for postglacial mire formation. *Geografiska Annaler: Series A, Physical Geography*, 100(3), 254–271. Available from: https://doi.org/10.1080/04353676.2018.1446638

Hagg, W. (2022) Glacial Sedimentation. In: *Glaciology and glacial geomorphology*. Berlin, Heidelberg: Springer. https://doi.org/10.1007/978-3-662-64714-1_11

Hansen, D.D. & Zoet, L.K. (2022) Characterizing sediment flux of deforming glacier beds. *Journal of Geophysical Research: Earth Surface*, 127(4), e2021JF006544. Available from: https://doi.org/10.1029/2021JF006544

Head, K.H. (1989) *Manual of soil laboratory testing, volume 1: soil classification and compaction tests*. London: Pentech Press.

Hooke, R.L. (2019) *Principles of glacier mechanics*. Cambridge: Cambridge university press.

Kentula, M.E. (1989) Wetland creation and restoration: the status of the science. Corvallis Environmental Research Laboratory, Office of Research and Development, US Environmental Protection Agency.

Lambe, T.W. & Whitman, R.V. (1991) *Soil mechanics*, Vol. 10. New York, NY: John Wiley & Sons.

Lolos, D.N. (2013) Estimating Paleo Ice Volumes Beneath Collapse Kettles: A Case Study of John's Pond, Mashpee, Massachusetts.

Maizels, J. (1997) Jökulhlaup deposits in proglacial areas. *Quaternary Science Reviews*, 16(7), 793–819. Available from: https://doi.org/10.1016/S0277-3791(97)00023-1

Maizels, J.K. (1977) Experiments on the origin of kettle-holes. *Journal of Glaciology*, 18(79), 291–303. Available from: https://doi.org/10.3189/S0022143000021365

Mickelson, D.M., & Attig, J.W. (2017) Laurentide ice sheet: ice-margin positions in Wisconsin. Wisconsin Geological and Natural History Survey.

Vasić, F., Paul, C., Strauss, V. & Helming, K. (2020) Ecosystem services of kettle holes in agricultural landscapes. *Agronomy*, 10(9), 1326. Available from: https://doi.org/10.3390/agronomy10091326

Wisconsin elevation/lidar data. State Cartographer's Office. (2023). http://www.sco.wisc.edu/data/elevationlidar

Yansa, C.H., Fulton, A.E., Schaetzl, R.J., Kettle, J.M. & Arbogast, A.F. (2020) Interpreting basal sediments and plant fossils in kettle lakes: insights from Silver Lake, Michigan, USA. *Canadian Journal of Earth Sciences*, 57(2), 292–293. Available from: https://doi.org/10.1139/cjes-2018-0338

SUPPORTING INFORMATION

Additional supporting information can be found online in the Supporting Information section at the end of this article.

How to cite this article: Prescott, J.S., Zoet, L.K., Hansen, D.D., Penprase, S.B. & Rawling, J.E. III (2024) Controls on glacial kettle morphology. *Earth Surface Processes and Landforms*, 49(15), 5244–5253. Available from: https://doi.org/10.1002/esp.6030